(Invited) 2355

FLUORIDE PHOSPHATE AND PHOSPHATE GLASSES FOR PHOTONICS

H. EBENDORFF-HEIDEPRIEM
Optoelectronics Research Centre, University of Southampton, SO17 1BJ, U.K.

Abstract Phosphate (P) and fluoride phosphate (FP) glasses are attractive materials for a wide range of photonic applications such as lasers, amplifiers, photosensitivity, optical storage and Faraday rotators. They demonstrate high UV transmission, low linear and nonlinear refractive index, low viscosity and low melting temperatures, athermal behaviour. In addition, they are excellent host materials for active rare earth (RE) ions due to advantageous local structure effect and high RE ion solubility. The paper reviews the benefit of FP and P glass properties for different photonic applications. Base glass properties, local structure and its effect on RE ion properties are described for FP and P glasses studied by the author. The potential of the glasses for laser, amplifier and photosensitivity-based devices are demonstrated.

INTRODUCTION

The field of photonics comprises the generation, transmission and detection of light as carrier of information and energy. Photonics is a future technology of growing importance with widespread applications in telecommunications, medicine, biology, research and sensing. Rare earth (RE) ions are widely used as active ions.

Due to their suitable combination of properties, fluoride phosphate (FP) and phosphate (P) glasses are attractive host materials for a variety of photonic devices such as high power lasers, fibre and waveguide amplifiers, optical isolators, photosensitivity-based devices, phosphors, scintillators and optical storage devices.

The high UV transparency of FP and P glasses enables the exploitation of different electronic transitions of active ions situated in the UV spectral range such as 4f-5d and charge transfer (CT) absorption and emission bands of polyvalent RE ions. These transitions are used in Faraday rotators[1], photostimulable phosphors for x-ray dosimeters[2], optical storage devices based on spectral hole burning[3] and gratings imprinted by UV laser exposure[4]. Another benefit of high UV transmission is the low

damage by UV lasers, which in turn is the precondition for the design of core-cladding-devices where the photosensitivity is confined to the core such as in fibre Bragg gratings[5].

FP and P glasses have low refractive indices in the range of 1.4-1.6 (Tab. 1) depending on fluoride and heavy metal ion content. Low refractive index comparable with silica facilitates index matching to standard telecom fibres and to silica-based planar devices. Otherwise, they give rise to high fluorescence lifetimes of RE laser ions, resulting in high gain for lasers and amplifiers[6]. The low nonlinear refractive indices minimize self-focusing of the laser beam, which can lead to catastrophic damage in high power lasers[6].

Compared with silicate glasses, FP and P glasses have low melting temperatures and viscosities[7], resulting in convenient process temperatures for device fabrication such as rotational casting, extrusion, fibre drawing. Another benefit is the fast achievement of different redox states[7] and in conjunction with this the creation of lower valent RE ions[8,9], which are the active dopants in Faraday rotators[1], photostimulable phosphors for x-ray dosimeters[2], optical storage devices based on spectral hole burning[3] and gratings imprinted by UV laser exposure[4]. P glasses with sodium content of ≥6mol% Na_2O are suitable for fabrication of ion-exchanged waveguide devices using potassium or silver salts.[10]

The high RE solubility in FP and P glasses is essential for Faraday rotators[1], scintillators[11] and compact devices with very short active lengths[6,10]. The local structure of the glasses affects the laser properties of the RE ions. In dependence of the composition, they are attractive hosts for different laser and amplifier applications as presented below.

Many FP and P glasses demonstrate so-called athermal behaviour.[12] As a result of the negative temperature coefficient of the refractive index, the change of the optical path length with temperature is nearly zero or even negative. This feature together with the low stress optic coefficient of FP and P glasses enables minimizing beam distortion in high power lasers.[12]

The properties of FP glasses can be adjusted by the phosphate/fluoride content, providing a useful tool in the design of core-cladding-devices with somewhat different refractive index of core and cladding but similar expansion coefficients and

transformation temperatures. Furthermore, the adjustment of the local structure effect on RE ion properties is used in the design of laser and amplifier devices.

This paper provides a brief review on our investigations on FP and P glasses with the aim of developing RE doped devices for photonics. First, structure, properties and redox behaviour of the base glasses are presented. Selected relationships between local glass structure and RE ion properties are described. At last, the potential for certain laser, amplifier and photosensitivity applications is demonstrated. The experimental procedures for glass preparation and optical measurements are reported in Refs.[8,9,13-16].

PROPERTIES OF THE BASE GLASSES

Batch compositions and properties of the base glasses are listed in Tab. 1.

FP, metaphosphate and ultraphosphate glasses contain Q^n PO_4 tetrahedra, which differ in their number n of bridging oxygens. In FP glasses, mono- and diphosphate groups (Q^0 and Q^1) are bonded into chains of fluoroaluminates. Monophosphate groups are prevailing in FP03, whereas a high number of diphosphate groups are found in FP20. Metaphosphate glasses mainly consist of Q^2 groups, which form long polyphosphate chains. UP glasses exhibit a cross-linked phosphate network composed of Q^2 and Q^3 groups.[17]

The UV transmission of the glasses is limited by the intense absorptions due to Fe^{3+} and other impurities ions (Fig. 1). The intrinsic band gap edges are situated in the VUV spectral range.[17] The IR transmission is governed by the broad band of the OH fundamental vibration at 2500-3700 cm^{-1} and by overtones of P-O and Al-F vibrations (Fig. 1). Since OH groups increase the attenuation loss of optical fibres and decrease the fluorescence lifetimes of important RE laser transitions such as Nd^{3+} at 1.1 µm and Er^{3+} at 1.5 µm, their content should be as low as possible. Due to their high fluoride content, FP glasses exhibit low OH contents already under conventional melting conditions. In P glasses, the OH content can be minimized by using bubbling of dry oxygen through the glass melt.[14,15]

According to their UV absorption, the glasses melted under different conditions can be divided in 4 different redox states. The "air" state indicates that the main part of the impurity iron ions occur as higher valent Fe^{3+} (>50%), which is demonstrated by the pronounced Fe^{3+} CT band at about 250 nm. The high UV absorption <220 nm originates

from the Fe^{3+} CT band at 185 nm[7] (Fig. 2). In FP and UP glasses, the "air" redox state is observed in the glasses obtained by batch melting in ambient atmosphere. In SrMP glass, this state is achieved only after remelting as shown below. In the reduced glasses designated with "red", almost all iron ions occur in the lower valent state Fe^{2+} (>99%).[7] The Fe^{3+} band at 250 nm is vanished and the UV absorption <220 nm is lower compared with "air" glasses. In FP glasses, the "red" state is achieved by remelting the starting glasses in carbon crucibles in argon atmosphere. In SrMP, the "red" state is already obtained by batch melting due to inorganic impurities in the raw materials used. After remelting of these starting glasses in ambient atmosphere, the "air" state is reached. In UP glasses, different reducing melting conditions (remelting in carbon crucibles in argon atmosphere, use of sugar and aluminium as reducing agents) did not result in a reduced glass comparable with FP/red and SrMP/red, but a more reduced state was achieved, which is designated with "red*". Characteristic feature of this state is the higher UV absorption <210 nm compared with the "red" glasses, which leads to a shift of the UV edge. In SrMP glass, the "red*" state is achieved by use of sugar as reducing agent. The high UV absorption in the "red*" glasses is attributed to lower valent phosphorous species such as P^{3+} and indicates reduction of the phosphate component.[17] The "ox" state refers to oxidized glasses melted using oxygen bubbling through the melt. According to Ref.[7], a ratio of >90% $Fe^{3+}/\Sigma Fe$ is found in "ox" glasses. Oxygen bubbling causes a more or less pronounced absorption band at 220 nm in some P glass samples, which is attributed to oxygen species that are incorporated in the glass network.

TABLE 1. Batch compositions and properties of the base glasses: density, refractive index (n_e), transformation temperature (T_g), thermal expansion coefficient (α).

glass	composition (mol%)	density (g/cm^3)	n_e	T_g (°C)	α (10^{-7}/K)
FP03	3 $Sr(PO_3)_2$ – 97 [MF_2, AlF_3] {M=Mg,Ca,Sr}	3.47	1.42	420	
FP10	10 $Sr(PO_3)_2$ – 90 [MF_2, AlF_3] {M=Mg,Ca,Sr}	3.44	1.46	440	160
FP20	20 $Sr(PO_3)_2$ – 80 [MF_2, AlF_3] {M=Mg,Ca,Sr}	3.54	1.50	480	150
SrMP	100 $Sr(PO_3)_2$	3.16	1.56	495	125
KLaMP	40 KPO_3 – 60 $La(PO_3)_3$	3.12	1.57	515	
KBaMP	35 KPO_3 – 40 $Ba(PO_3)_2$ – 20 $Al(PO_3)_3$ – 5 BaF_2	3.09	1.55		130
UP	50 $M(PO_3)_2$ – 14 $Al(PO_3)_3$ – 36 P_2O_5 {M=Mg,Ca,Ba,Zn}	2.83	1.54	460	105

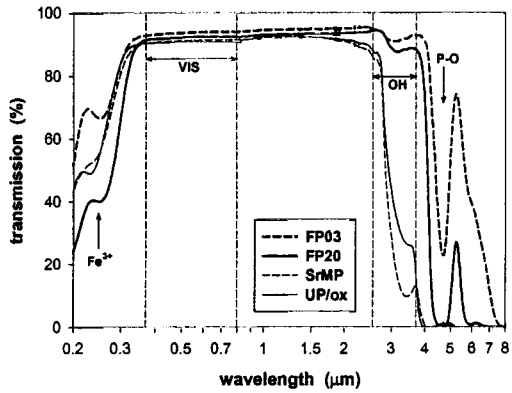

FIGURE 1. Transmission spectra of glass samples having 2 mm thickness.

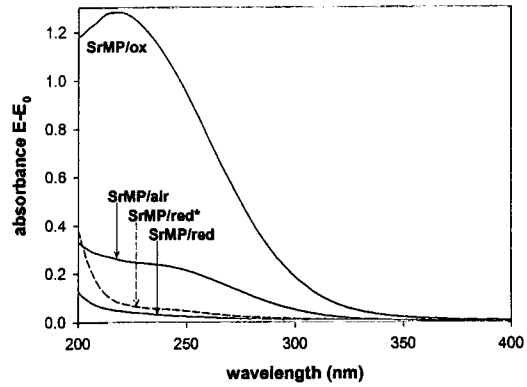

FIGURE 2. UV absorption spectra of SrMP glass samples having 2 mm thickness.

LOCAL GLASS STRUCTURE AND ITS EFFECT ON RE ION PROPERTIES

The spectroscopic properties of 4f-5d and CT transitions are used to reveal the local structure around RE ions as well as to study the redox behaviour of RE ions. The lower valent ions Eu^{2+}, Ce^{3+} and Tb^{3+} demonstrate 4f-5d absorption bands, whereas the higher valent ions Eu^{3+}, Ce^{4+} and $(Tb^{3+})^{+}$ show CT absorption bands in the UV region (≥190 nm) measurable by conventional spectrophotometers. Separation and assignment of the bands are described in Ref.[8]. The peak wavelength of the first low-energy 4f-5d band act as a suitable measure for the barycentre of the 4f-5d energy difference. Equally, the oscillator strength of the first 4f-5d band exhibits the same compositional dependence as the one of all 4f-5d bands. The compositional dependence of the first 4f-5d band is similar for the three RE ions studied, Tb^{3+}, Ce^{3+}, Eu^{2+}. This behaviour justifies that general conclusions on local structures around RE ions can be obtained using one RE ion as an example. For this purpose, Tb^{3+} is a very suitable indicator ion since its first 4f-5d band is clearly separated in all the glasses studied. Furthermore, Tb^{3+} is the only redox state of terbium in glasses melted under conventional conditions. Properties of RE CT transitions are studied in detail for Eu^{3+} as an example.[8]

The peak wavelength of the Tb^{3+} 4f-5d absorption band reflects the delocalisation of the electron cloud of RE ions towards the ligands. Thus, it is a suitable measure for the covalency between RE ions and ligands. The polarisability of all ligands determines the degree of covalency. Growing phosphate content from FP to metaphosphate glasses as well as increasing amount of non-bridging oxygens (NBO) from UP to metaphosphate glasses result in a higher covalency of the RE coordination polyhedra.[8]

The peak wavelength of the Eu^{3+} CT absorption band reflects the electron donor power of ligands towards the RE ions. The different compositional dependence of 4f-5d and CT peak wavelengths (Fig. 3) suggests that the electron donor power and polarisability of the ligands are not affected in the same manner. In FP glasses, the high electron donor power of the oxygen ions is considered to dominate over the low one of fluorine ions. Clearly different shape of RE 4f-5d absorption spectra in FP glasses compared with P glasses indicates that the mixed anion environment in FP glasses leads to a different geometric arrangement of the ligands[8], which is assumed to be a further reason for the high CT peak wavelengths in FP glasses compared to P glasses (Fig. 3).

The oscillator strengths of 4f-5d and CT bands provide information about the asymmetry of the RE ion polyhedra, which increases the more rigid the glass network. The rigidity is governed by bond type and degree of linkage in the glass matrix. In the FP and metaphosphate glasses, covalency and asymmetry change in the same manner. UP glass, however, show a very high asymmetry in relation to covalency.[8]

The redox behaviour of RE ions is studied for polyvalent europium and terbium ions. The formation of Eu^{2+} ions can be easily monitored by their intense 4f-5d band at 250 nm. Radiation-induced oxidation of Tb^{3+} ions can be recorded by emergence of the intense $(Tb^{3+})^{+}$ CT band and decrease of the sharp Tb^{3+} 4f-5d band at 210 nm.[9] In FP glasses, up to 30% Eu^{2+} ions relative to the whole europium ion concentration (ΣEu) are formed by chemical reduction. In SrMP glass, only a small number of Eu^{2+} ions (2%) is generated. In UP glasses, no Eu^{3+} ions but P(V) atoms are reduced. This suggests that in FP glasses Eu^{3+} ions are more easily reduced than P(V) species, whereas an opposite behaviour is observed in UP glasses. On the other side, formation of higher valent $(Tb^{3+})^{+}$ ions under x-ray irradiation is favoured in UP glasses [$(Tb^{3+})^{+}/\Sigma$Tb ratio: 5% in FP10 – 7% in SrMP – 10% in UP]. The tendency of Eu^{2+} and $(Tb^{3+})^{+}$ formation correlates with the Eu^{3+} CT energy. Both Eu^{2+}/ΣEu ratio and CT peak wavelength decrease in the order FP10-SrMP-UP, whereas the $(Tb^{3+})^{+}/\Sigma$Tb ratio increases. This demonstrates that the electron donor power of ligands has an important influence on the redox behaviour of RE ions.

The Ω_6 Judd-Ofelt parameter, which determines the intensity of important laser transitions such as Nd^{3+} at 1.1 μm and Er^{3+} at 1.5 μm, depends on the electron donor power of the ligands. Interaction with the 6s and 5d orbitals of RE ions demonstrate

opposite behaviour.[18] The former decreases but the latter increases Ω_6. In P glasses, increasing covalency (indicated by increasing 4f-5d peak wavelength) coincides with increasing electron donation in the 6s orbital, resulting in decreasing Ω_6 (Fig. 4). The high Ω_6 parameter of FP glasses indicates high electron donor power towards the 5d orbitals of RE ions, which grows as the phosphate content increases. The different local structure effect on Ω_6 in FP and P glasses correlates with the different local structure effect of both glass types on the CT energy.

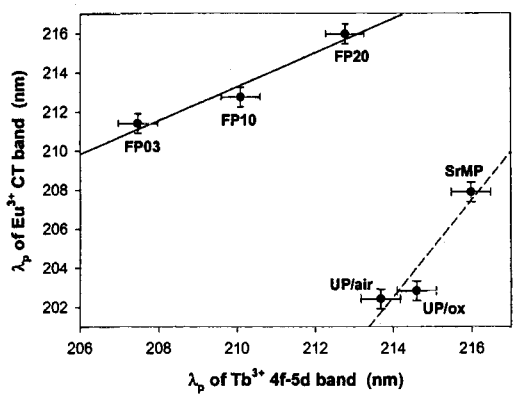

FIGURE 3. Peak wavelength of Tb^{3+} 4f-5d absorption as a function of the one of Eu^{3+} CT absorption.

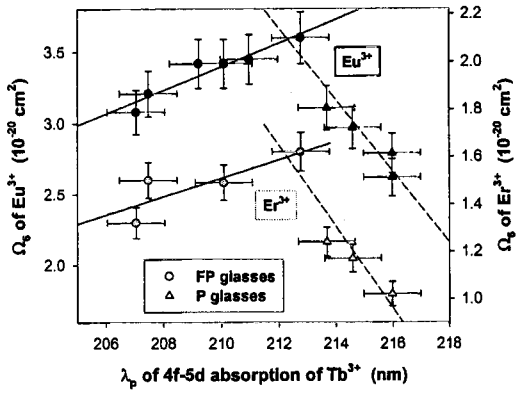

FIGURE 4. Ω_6 Judd-Ofelt parameter as a function of Tb^{3+} 4f-5d peak wavelength.

Phonon sideband measurements of Eu^{3+} excitation spectra reveal that in FP glasses solely the high-energy phonons of diphosphate groups couple with the RE electrons. In P glasses symmetric and asymmetric vibrations participate in the electron-phonon-coupling. As the covalency increases from FP to SrMP glasses, coupling between RE electrons and host glass phonons becomes stronger (Tab. 2). Thus, the multiphonon relaxation rate of RE ions increases from FP03 to FP20 despite equal phonon energy. The increase of the Er^{3+} fluorescence intensity at 1.5 μm with the phosphate content in FP glasses is ascribed to increasing population of the upper fluorescence level by enhancement of multiphonon decay from upper energy levels. The high multiphonon relaxation rate in P glasses results from both high electron-phonon-coupling strength and high phonon energy.[13]

Decrease of RE ion fluorescence lifetimes by cross relaxation and OH quenching is studied for Tb^{3+} $^5D_3$-$^7F_6$, Nd^{3+} $^4F_{3/2}$-$^4I_{11/2}$ and Er^{3+} $^4I_{13/2}$-$^4I_{15/2}$ emissions.[13,15] For Nd^{3+} and Er^{3+}, the rate of energy migration between the RE ions is much higher than the one of

cross relaxation and energy transfer to OH groups, resulting in enhanced quenching process at higher RE concentrations $>1\times10^{20}$ ions cm^{-3}. In P glasses, where OH quenching is a crucial point, modelling of the fluorescence decay curves shows that OH quenching occurs even at very low RE concentrations. This phenomenon indicates clustering of RE ions and OH groups. Both species prefer coordination with NBO. Energy transfer microparameters are determined by oscillator strengths and spectral overlap of donor and acceptor transitions. Thus, the compositional dependence of the Nd^{3+} and Tb^{3+} cross relaxation microparameters (Tab. 2) results from the local structure effect on the Ω_t intensity parameters and on the linewidths of the involved transitions. The clearly lower microparameters in KLaMP glass compared with FP20 glass are caused by both lower Ω_6 parameters and narrower bands.[13]

TABLE 2. Spectroscopic properties of RE ions: electron-phonon-coupling strength (g), microparameters of direct donor-acceptor energy transfer (C) and of energy migration enhanced transfer (C'), effective linewidth ($\Delta\lambda_{eff}$), stimulated peak emission cross section ($\sigma_{e,p}$) calculated radiative (τ_{rad}) and observed fluorescence (τ_{obs}) lifetimes.

glass	g (10^{-3})	microparameters (10^{-40} s/cm^6)				Er^{3+} transition at 1.5 µm			
		C_{Tb-Tb}	C'_{Nd-Nd}	C_{RE-OH}	C'_{RE-OH}	$\Delta\lambda_{eff}$ (nm)	$\sigma_{e,p}$ (10^{-20} cm^2)	τ_{rad} (ms)	τ_{obs} (ms)
FP03	2.2	5.2				68	6.3*	8.6	
FP10	6.0	6.3							
FP20	8.6	7.6	6.7	6.8 (Tb)	18 (Nd)	65	7.5	6.8	9.8
SrMP	17.4	5.1	3.0						
KLaMP		3.3	1.0						
KBaMP						48	7.9	8.5	6.0
OX						47	6.9		7.9
UP		6.8		2.4 (Er)	5.5 (Er)	46	9.3	7.8	8.7

*calculated from absorption spectra using McCumber theory[15]

LASER PROPERTIES OF ER3+ AT 1.5 µm

Important laser properties are fluorescence lifetime, linewidth and peak emission cross section, $\sigma_{e,p}$, of the laser transition (Tab. 2). For Er^{3+} transition at 1.5 µm, the latter parameter in turn depends on linewidth, refractive index and Ω_6 parameter. FP glasses show clearly broader and flattened lineshape of Er^{3+} transition at 1.5 µm than P glasses

due to mixed anion coordination. The UP glass has a high $\sigma_{e,p}$ value as a result of the very small linewidth. The high $\sigma_{e,p}$ value of FP20 originates from the high Ω_6 parameter.

Laser experiments were carried out with FP20, UP and commercial QX metaphosphate glass samples.[15,19] Laser oscillation was observed for all three glass types. The laser tuning range was measured for the FP20 and the QX glass (Fig. 5). The FP20 glass demonstrates a very broad band ranging from 1505 to 1600 nm. The laser output is flattened between 1535 and 1585 nm. By contrast, the laser spectrum of the QX glass consists of a sharp peak ranging only from 1533 to 1555 nm. The lower output and higher threshold of the FP20 glass corresponds with the lower emission cross section at 1560 nm in the FP20 glass compared with the high peak emission cross section at 1533 nm in the QX glass. The UP samples show lower output and higher threshold than the QX glass due to low optical quality and occurrence of OH quenching. Thus, further improvement of glass fabrication is necessary.

The broad and flattened laser tuning spectrum connected with a relatively high laser output make the FP20 glass a very attractive candidate for broadband amplifiers in telecommunications. Because of their high peak emission cross sections, ultraphosphate glasses have potential for high energy/high peak power lasers.

PHOTOSENSITIVITY OF EU2+ DOPED FP GLASS

Eu^{2+} doped FP10 glasses fabricated by reducing melting conditions proved to be photosensitive.[16] By direct UV laser writing at 244 nm, waveguides clearly visible by launching light of a fibre-coupled HeNe laser at 633 nm have been created for different UV laser powers and writing scan speeds (Fig. 6). The disappearance of the Eu^{2+} absorption at 250 nm after laser irradiation at 244 nm and 248 nm indicates complete photooxidation of Eu^{2+}. The intense UV absorption simultaneously induced is attributed to electron defect centres formed in conjunction with photooxidation. No recovery of the absorption was observed after annealing up to 400 °C. This suggests high thermal stability of photosensitivity in Eu^{2+} doped FP glasses.

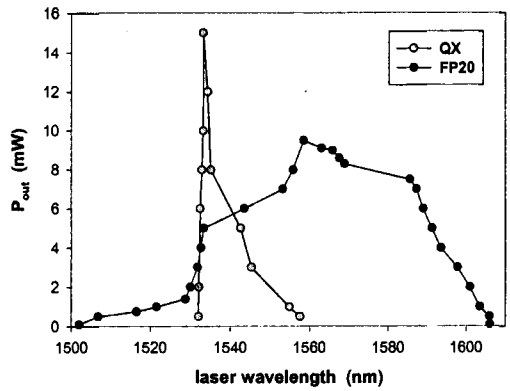

FIGURE 5. Laser tuning spectra of QX® metaphosphate glass (1.4×10^{19} Er^{3+} cm^{-3}, 16×10^{20} Yb^{3+} cm^{-3}) and FP20 glass (5×10^{19} Er^{3+} cm^{-3}, 8×10^{20} Yb^{3+} cm^{-3}).

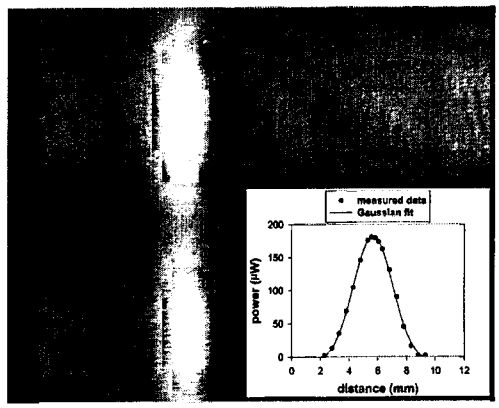

FIGURE 6. Near-field image of a waveguide written by UV laser at 244 nm in Eu^{2+} doped FP10 glass. The inset shows the far-field mode-profile.

ACKNOWLEDGEMENT

The author wish to thank D. Ehrt, U. Natura, P Ebeling and coworkers (Otto-Schott-Institut, University of Jena, Germany); J. Philipps, T. Töpfer (Institut für Optik und Quantenelektronik, University of Jena, Germany); M. Bettinelli and A. Speghini (University of Verona, Italy); C. Riziotis and E.R. Taylor (Optoelectronics Research Centre, University of Southampton, U.K.) for their kind help with glass preparation, measurements and discussions. The work was funded by Deutsche Forschungsgemeinschaft, Thüringer Ministerium für Wissenschaft, Forschung und Kunst and Schott Glass company in Germany. The author is also grateful to the EU for financial support by Marie Curie Individual Fellowship.

REFERENCES

1. M. Yamane, Y. Asahara, Glasses for photonics, (Cambridge University Press, 2000)
2. J. Qiu, J. Ceram. Soc. Japan, 109, S25 (2001)
3. K. Hirao, J. Non-Cryst. Solids, 196, 16 (1996)
4. T. Taunay, P. Bernage, M. Douay, W.X. Xie, et al., J. Opt. Soc. Am., B 14, 912 (1997)
5. A. Othonos, Rev. Sci. Instrum., 68, 4309 (1997)
6. M.J. Weber, J. Non-Cryst. Solids, 123, 208 (1990)
7. D. Ehrt, M. Leister, A. Matthai, Molten Salt Forum, 5-6, 547 (1998)
8. H. Ebendorff-Heidepriem, D. Ehrt, Opt. Mater., 15, 7 (2000)
9. H. Ebendorff-Heidepriem, D. Ehrt, Phys. Chem. Glasses, to be published
10. S. Jiang, T. Luo, B.-C. Hwang, G. Nunzi-Conti, et al., Opt. Eng., 37, 3282 (1998)
11. S. Baccaro, A. Cecilia, A. Cemmi, G. Chen, et al., IEEE Trans. Nucl. Sci., 48, 360 (2001)
12. J.E. Marion, M.J. Weber, Eur. J. Solid State Inorg. Chem., 28, 271 (1991)
13. H. Ebendorff-Heidepriem, D. Ehrt, Glastech. Ber. Glass Sci. Technol., 71, 289 (1998)
14. H. Ebendorff-Heidepriem, D. Ehrt, M. Bettinelli, A. Speghini, Proc. SPIE, 3622, 19 (1999)
15. H. Ebendorff-Heidepriem, D. Ehrt, J. Philipps, T. Töpfer, et al., Proc. SPIE, 3942, 29 (2000)
16. H. Ebendorff-Heidepriem, C. Riziotis, E.R. Taylor, Proc. 6th ESG Conference, (France 2002)
17. D. Ehrt, P. Ebeling, U. Natura, J. Non-Cryst. Solids, 263&264, 240 (2000)
18. S. Tanabe, T. Hanada, T. Ohyagi, N. Soga, Phys. Rev., B 48, 10591 (1993)
19. J.F. Philipps, T. Töpfer, H. Ebendorff-Heidepriem, D. Ehrt, et al., Appl. Phys., B 72, 399 (2001)